Journal of Power Sources 248 (2014) 969–977

Contents lists available at ScienceDirect

Journal of Power Sources

journal homepage: www.elsevier.com/locate/jpowsour

Impact of Solid Electrolyte Interphase lithium salts on cycling ability of Li-ion battery: Beneficial effect of glymes additives

Fabien Chrétien [a], Jennifer Jones [a], Christine Damas [a], Daniel Lemordant [a], Patrick Willmann [b], Mériem Anouti [a,*]

[a] Université François Rabelais, Laboratoire PCM2E (EA 6299), Parc de Grandmont, 37200 Tours, France
[b] CNES, 18 Avenue Edouard Belin, 31055 Toulouse, France

HIGHLIGHTS

- Addition of glyme does not have strong impact on iconicity.
- LiOH, LiF and Li_2O have detrimental impact upon cycling.
- Li_2CO_3, $LiOCH_3$ and $LiOC_2H_5$ form a steady SEI.
- Glymes compounds and LiF together have better impact than each one separately.

GRAPHICAL ABSTRACT

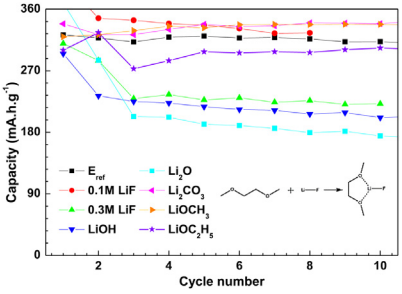

ARTICLE INFO

Article history:
Received 20 July 2013
Received in revised form
6 September 2013
Accepted 16 September 2013
Available online 5 October 2013

Keywords:
SEI
Lithium salt
Batteries
Graphite
NMC
Glymes

ABSTRACT

The Solid Electrolyte Interphase (SEI), formed during the first cycles of life in lithium-ion batteries, contains a variety of lithium salts, with direct effect on the aging performance of the battery. In this work, we investigate the impact of addition of SEI lithium salts (LiF, Li_2CO_3, LiOH, Li_2O, $LiOCH_3$ and $LiOC_2H_5$) in the electrolyte on the cycling ability of graphite and $LiNi_{1/3}Mn_{1/3}Co_{1/3}O_2$ (NMC) electrodes. Results show that NMC is more sensitive to salt addition than graphite material. Furthermore, results demonstrate that both LiOH and Li_2O have a negative effect on the SEI formation. Conversely, Li_2CO_3, $LiOCH_3$ and $LiOC_2H_5$ are beneficial and promote the formation of a polymeric coating on the SEI. Finally, the impact of the presence of LiF on the SEI depends mainly on its concentration. The effect of the presence of additives capable of complexing lithium salts such as the glyme series, $CH_3O[CH_2CH_2O]_nCH_3$ (G_n, with $n = 2$, 3 or 4), is investigated by cyclic voltammetry, galvanostatic charge–discharge tests and electrochemical impedance spectroscopy (EIS). Results show that the glymes chain length is a determining factor in their complexation mechanism, which depends on both the nature and the concentration of the lithium salt.

1. Introduction

Lithium ion batteries have been commercialized for two decades and technologies involved in these batteries (electrode materials, electrolyte and separators) are still under improvement to enhance their performance and stability. It is now admitted that efficient cycling of lithium-ion batteries is associated with the formation of a Solid Electrolyte Interphase (SEI) [1]. The composition and quality of this film is decisive for battery performance [2]. During the first cycles, several lithium salts are formed by reduction of electrolyte and/or degradation of lithium salts. Some of these lithium compounds contribute to the quality of the SEI which protects the electrode and improves battery aging. A way of improvement is to make the thinnest, most flexible and electrochemically stable SEI. It is known that the SEI

* Corresponding author. Tel.: +33 (0)247366951; fax: +33 (0)247367073.
E-mail address: meriem.anouti@univ-tours.fr (M. Anouti).

0378-7753/$ – see front matter © 2013 Elsevier B.V. All rights reserved.
http://dx.doi.org/10.1016/j.jpowsour.2013.09.092

is composed of mineral and organic lithium salts, mainly of Li_2CO_3, as well as, small quantities of nanometric LiF [3,4]. The predominance of these lithium species in the SEI has been widely described [3,5–16]. The impact of SEI salt components on the battery performance is still unclear: some species, such as LiF, are claimed to be detrimental to cycling, while some others such as lithium carbonate are beneficial to the battery performances [17,18]. But so far, no comprehensive study has been carried out to corroborate these assertions.

In this work, we investigate the role of SEI species on cycling by adding to the electrolyte diverse lithium salts present in the SEI to determine their influence on battery efficiency. Lithium salts selected for this study are lithium fluoride LiF, lithium carbonate Li_2CO_3, lithium hydroxide LiOH, lithium oxide Li_2O, lithium methoxide $LiOCH_3$ and lithium ethoxide $LiOC_2H_5$. Indeed, these compounds are present in the SEI when graphite and $LiNi_{1/3}Mn_{1/3}Co_{1/3}O_2$ (NMC) are used as electrodes with $LiPF_6$ 1 mol L^{-1} in EC/PC/3DMC (w/w) as electrolyte [19]. In this work, focus was made on LiF because of its preponderance within the SEI and its high solubility in EC/PC/3DMC (0.35 mol L^{-1} [5]) compared to the very low solubility of other lithium compounds in the same solution. One way to limit the effect of these salts on the battery performances is to complex them using additive agents, which prevent salts aggregation and precipitation in solution. Glymes compounds, $CH_3O(CH_2CH_2O)_nCH_3$ (G*n*, with $n = 2$, 3 or 4), are described in the literature as interesting additives or co-solvents able to complex lithium salts in solution [20,21]. Complexes formed between lithium salts and glymes are more electrochemically stable than ethers. Their high oxidation potential allows using them in batteries with NMC electrodes: value close to 4.7 V is reported in the case of the G2 glyme in the solution (EC/G2 + $LiPF_6$ or $LiClO_4$) [20], as potential value close to 4.6 V is claimed for the (G4 + LiBOB) mixture [22], and interestingly potentials higher than 4.5 V were reported in the case (G2, G3 or G4 glyme + LiTFSI) mixtures [23,24]. Herein, we decided to focus the purpose of this study on the utilization of glymes as electrolyte additives to enhance the battery cyclability in presence of high amount of lithium salts omnipresent in the SEI using graphite and NMC electrode materials.

2. Experimental

2.1. Materials

All solvents, ethylene carbonate (EC), dimethyl carbonate (DMC), propylene carbonate (PC), diethyleneglycol dimethyl ether (G2), triethyleneglycol dimethyl ether (G3), tetraethyleneglycol dimethyl ether (G4) were purchased from Sigma Aldrich (purity > 99%) and kept inside desiccant bags (Distribio – Genecust) to reduce the amount of residual water (less than 20 ppm after drying). Lithium salts $LiPF_6$, LiF, Li_2O, LiOH, Li_2CO_3, $LiOCH_3$ and $LiOC_2H_5$ were purchased from Sigma Aldrich and used without further purification. Additionally, prior to any measurement, electrolytes were analyzed for water content using coulometric Karl-Fischer (Coulometer 831 – Metrohm) titration. The water content of selected electrolytes is lower than (20 ± 1) ppm. Electrolyte solutions were then prepared in a glove-box (M-Braun) filled with Argon (H_2O < 5 ppm), by adding the appropriate weight of lithium salt LiX or glyme (G*n*, $n = 2$, 3 and 4) to the EC/PC/3DMC (w/w) + 1 M $LiPF_6$ electrolyte denoted E_{ref}.

2.2. Measurements

Ionic conductivities were obtained with a Crison (GLP31) digital multi-frequency conductometer. The cell constant of the electrode was calibrated using a 1 M $LiPF_6$ solution in EC/PC/3DMC ($\sigma = 12$ mS cm^{-1} at 25 °C) and the temperature was controlled from 20 °C to 60 °C ($\Delta T \pm 0.2$ °C). Viscosity and density measurements were conducted using an Anton Parr digital vibrating tube densitometer (model 60/602, Anton Parr, France) and an Anton Parr rolling-ball viscometer (model Lovis 2000 M/ME, Anton Parr, France), respectively. In both cases, the temperature in the cell was regulated within ±0.02 °C. The uncertainty of the density and viscosity measurements were better than 5×10^{-5} g cm^{-3}, and 1%, respectively.

Galvanostatic charge–discharge experiments and cyclic voltammetry were performed using a Versatile Multichannel Potentiostat MPG2 (Biologic S.A) piloted by an Ec Lab V10.20 interface.

Graphite and NMC electrodes were kindly provided by SAFT, active material masses of electrodes are equilibrated for the full cell system.

Charge–discharge and voltammetric cycling tests were conducted by using a three-electrodes configuration. The electrochemical full cell was built with a Teflon® Swagelok® system. Graphite and NMC disc electrodes coated respectively on copper and aluminum current collectors (diameter: 10 mm) were used as negative and positive electrode respectively and a Li foil as reference electrode. Porous polypropylene membrane (thickness: 25 μm, pore diameter: 0.2–0.5 μm) filled with the electrolyte solution was used as separator; constant pressure applied on electrode into three-electrodes Swagelok cell is 0.19 N mm^{-2}. The first cycle of each cell is performed at 60 °C to improve the SEI formation. Charge and discharge cycles were carried out in the galvanostatic mode at C/10 rate. Cycling was operated between 3 V and 4.2 V for NMC and between 0.01 V and 2.0 V for graphite. Electrochemical stability tests on glymes were carried out with a platinum disc (diameter 2 mm) as working electrode, a lithium metal disc as counter electrode and a lithium foil as reference electrode. Electrochemical impedance spectroscopy (EIS) measurements on the cells were performed with a VMP3 (Biologic), with frequency sweep from (10^6 to 10^{-2}) Hz and a 10 mV sinusoidal signal.

3. Results and discussion

3.1. Physico-chemical properties of electrolytes

Physico-chemical characteristics of studied glymes at 25 °C are listed in Table 1.

Viscosities values of (2.09 and 3.69) mPa s reported at 25 °C, respectively for G3 and G4 are similar to those reported for carbonate solvents as PC (2.53 mPa s at 25 °C) or EC (1.90 mPa s at 40 °C), while G1 viscosity is very low (0.46 mPa s) as that of DMC (0.59 mPa s). G1 appears to be a good potential additive to decrease the electrolyte viscosity. However, its flash point (−6 °C), boiling point (85 °C) and quite high vapor pressure (72 mbar at 25 °C) do not allow to consider its use for battery application. For example, other glymes like G2, G3 and G4 have lower vapor pressure (12, 2.7

Table 1
Physico-chemical properties (molecular weight, melting point, boiling point, flash point, viscosity, relative permittivity and density) of selected glymes at 25 °C.

Properties	Mw [g mol^{-1}]	m.p [°C]	b.p [°C]	f.p [°C]	η^a (20 °C) [mPa.s]	ε_r	ρ^a (20 °C) [g cm^{-3}]
Monoglyme (G1)	90.12	−58	85	−6	0.46	5.5	0.874
Diglyme (G2)	134.17	−64	162	57	1.03	5.8	0.951
Triglyme (G3)	178.22	−45	216	111	2.09	7.5	0.993
Tetraglyme (G4)	222.28	−29.7	275	141	3.69	7.9	1.019

[a] Measured values.

and 0.7 mbar at 25 °C, respectively) than G1 but still higher that reported for PC (0.17 mbar). G2 seems to exhibit a good compromise between these properties: quite high large liquid temperature range driven by a low melting temperature (−64 °C) and high boiling point (162 °C), with a flash point close to 57 °C, and a viscosity of 1.03 mPa s at 20 °C. Furthermore, the dielectric constant of selected glymes varies from 5.5 to 7.9 at 25 °C, close to that reported in the case of DMC ($\varepsilon_r = 6$). However, these dielectric constant values are not favorable to the dissociation of lithium salt by comparison to very dissociating alkyl carbonates like EC and PC with $\varepsilon_r = 89$ (at 40 °C) and $\varepsilon_r = 64$ (at 25 °C), respectively.

In this study, EC/PC/3DMC (w/w) + 1 M $LiPF_6$ was used as reference electrolyte (denoted E_{ref}), as well as, its mixtures with glymes (G2, G3, or G4) or lithium salts LiX (LiF, Li_2CO_3, LiOH, Li_2O, $LiOCH_3$ and $LiOC_2H_5$). The effect of glymes on E_{ref} transport and volumetric properties was investigated by measuring the evolution of conductivity, viscosity and density of the mixtures (E_{ref} + G2) against molar fraction of G2 from 20 °C to 60 °C as shown in Fig. 1a–d. Theses variations are then compared to those obtained in the presence of 0.3 M LiF in E_{ref}. This choice is motivated, as mentioned in above, by the preponderance of lithium fluoride salt in the SEI and its high solubility in EC/PC/3DMC (w/w) by comparison with other lithium salts present at the interphase.

We can see on Fig. 1a that the conductivity (σ) varies linearly from (12 to 13.5) mS cm^{-1} when G2 is added to E_{ref} up to 12% in G2 mole fraction unit. This variation is consistent with that reported by Christie et al. in the case of the addition of G2 in the electrolyte based on $LiPF_6$ dissolved in PC [25]. By adding 0.3 M LiF in E_{ref}, σ is maximum at a G2 mole fraction close to 6%, beyond this composition the G2 addition effect on conductivity is negligible. When we express the variation of the conductivity as a function of the r ratio ($r = n_{Li}/n_{G2}$), where n_{Li} and n_{G2} are respectively the number of moles of Li (from $LiPF_6$ and LiF) and of G2, there is an initial decrease on conductivity up to $r = 2$, then the conductivity remains constant, as shown in Fig. 1b. The effect of the presence of G2 and/or LiF on the electrolyte density can be evaluated with Fig. 1c at different temperatures, from which it appears that both G2 and LiF have also an impact on this property. The density of the solution decreases with the G2 and/or LiF concentrations in the solution. Additionally, the density of each solution decreases, as expected, with the temperature. As shown in Fig. 1d, the addition of a rather low viscous glyme (G2, 1.03 mPa s at 20 °C) compared to that of E_{ref} (3.68 mPa s at 20 °C) leads effectively to a decrease in the viscosity of the solution. As expected, the viscosity of all solutions decreases with a temperature increase. Nevertheless, in contrast to the density, no difference was observed on the viscosity when G2 is added to E_{ref} in the presence or in absence of LiF.

In other words, the presence of LiF seems to have nearly no impact on transport properties, whereas G2 contributes to an increase in the electrolyte conductivity as the n_{Li}/n_{G2} ratio becomes lower than 2 approximately. This phenomenon is probably due to the ability of G2 to complex Li^+ ions as already described in the literature [25]. The G2 additive has oxygen atoms that act as potential chelating centers. Moreover the donor number (DN) value of G2 (21.3) is higher than those reported for PC, EC and DMC (range from 15.1 to 17.2). This can also explain favorable interactions between G2 molecules and acceptor sites such as lithium cation in LiF salt.

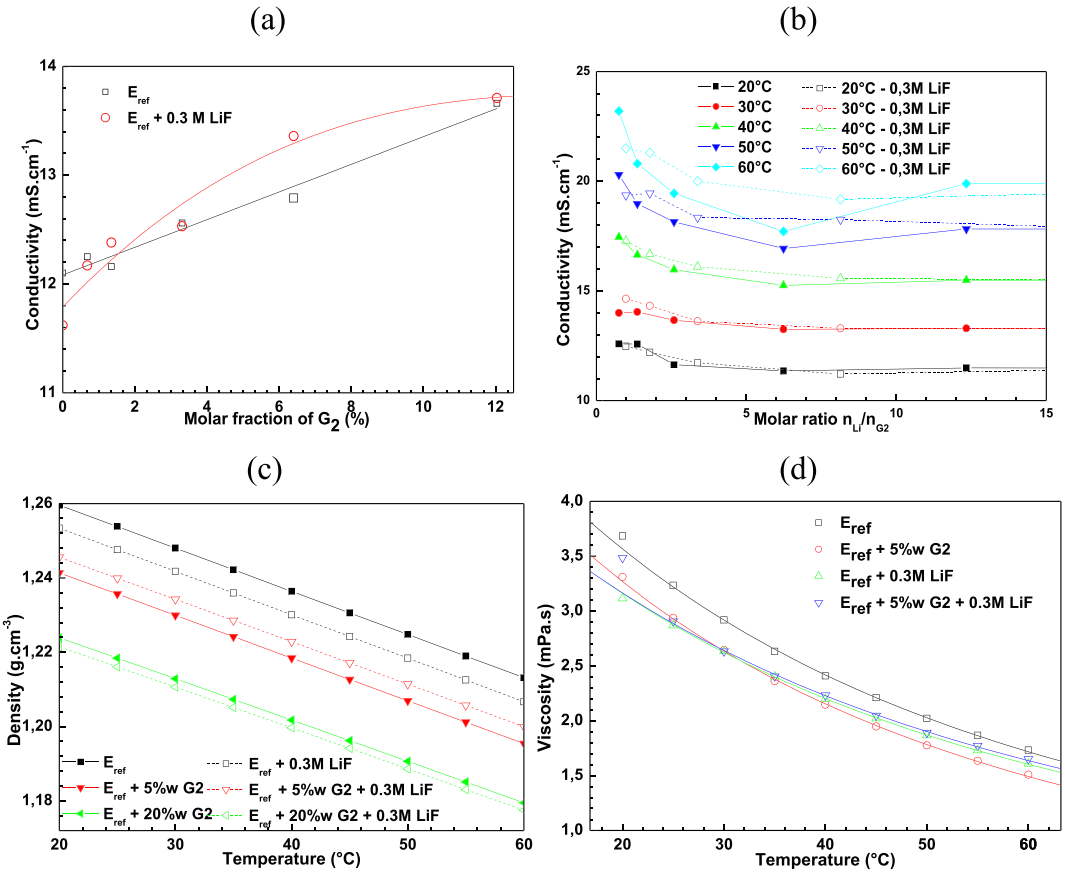

Fig. 1. Variation of physico-chemical properties of E_{ref} upon addition of G2 and/or 0.3 M LiF, (a) conductivity at 25 °C as a function of G2 mole fraction, (b) conductivity at various temperatures as a function of the molar ratio n_{Li}/n_{G2} (c) density as a function of temperature (d) viscosity as a function of temperature.

One way of assessing electrolytic ionicity is to use the classification diagram based on the classical Walden rule [26,27]. The Walden rule (Fig. 2) relates the ionic mobility represented by the equivalent conductivity Λ as a function of the fluidity η^{-1} of the medium through which the ions move. From Fig. 2, it appears that the addition of G2 and/or LiF to the E_{ref} electrolyte does not seem to have a strong impact on the Walden classification of solutions, e.g. on the relationship between viscosity and conductivity of these solutions. However, as shown in Fig. 2 insert, it appears that E_{ref} containing 20% in mass (denoted %w) of G2 and 0.3 M LiF is the most ionic mixture, as it is close to the ideal KCl line. However, if the G2 content is 5%w in E_{ref}, with or without the addition of LiF salt, solution is less ionic than the E_{ref} (e.g. points are moved below the E_{ref} curve). Accordingly, the presence of LiF does not seem to impact strongly the physico-chemical properties, which enables the assessment of the electrochemical properties of the E_{ref}.

3.2. Electrochemical aspect

3.2.1. Cyclability of graphite/NMC system in the presence of lithium salt

In the experiments described herein, solutions containing LiX (LiF, Li_2CO_3, LiOH, Li_2O, $LiOCH_3$ and $LiOC_2H_5$) are compared with LiX-free solutions based on the classical electrolyte based on the dissolution of 1 M $LiPF_6$ in the EC/PC/3DMC (w/w) solution used therein as the reference electrolyte. Measurements were therefore carried out in parallel using similar electrodes and solutions, as well as, the same instrumentation (i.e. two similar electrochemical work stations were always used simultaneously). Lithium salts studied herein have a very low solubility in PC/EC/3DMC [5]. Lithium salts were then introduced at saturation according to the solubility values reported previously [5]. LiF is thoroughly studied in this work because of its higher solubility comparatively to other lithium salts, its predominance and its resistive behavior toward Li^+ migration in the SEI. Cycling using a three-electrodes cell allows to study distinctly the behavior of each electrode. Indeed, reaction products formed at the surface of one electrode can migrate across the electrolyte and react at the other electrode, which cannot be evidenced in half-cell configuration.

Fig. 3 shows the voltammograms of graphite (blue and insert) and NMC electrodes (red in the web version) in E_{ref} in the absence of LiX. For graphite, the SEI formation at the first cycle from the electrolyte reduction at around 0.9 V is shown in Fig. 3 insert, and each step of lithium intercalation (A–E) is then visible. Phase compositions as described by J.R. Dahn [28] and values of potential for each electrochemical step are reported in Table 2. For NMC electrode (red curve in Fig. 3), the first cycle involves over-potential to initiate the de-insertion and insertion of lithium. Following cycles are similar to the second one. Considering the base line (black curve), electrochemical stability of G2 in E_{ref} at platinum electrode from 2 V to 4.4 V is also evident.

When considering the similar curves obtained under the same conditions in the presence of 0.3 M of LiF (Fig. 4), we observe a passivation layer formation at the same potential: 0.9 V vs. Li^+/Li. However, the insertion stages are completely disrupted and less marked than in absence of LiF, especially $(2+1)$ and $(2+2L)$ phases (see Table 2) corresponding to peaks D and E in Fig. 4. We also notify that intercalation/de-intercalation mechanisms are less reversible in the presence than in absence of LiF in solution. The irreversible processes (surface film formation) are faster than the Li insertion, and hence may be completed during relatively fast polarization. However, since the experiment conditions giving results reported in Figs. 3 and 4 are identical, it can be clearly reported that the presence of LiF increases the irreversible charge involved in the first cathodic process ($i = 0.05$ mA in E_{ref}, $i = 0.14$ mA in E_{ref} + LiF), which relates to the formation of a thick layer of passivation upon LiF addition. These observations suggest that the presence of LiF in the electrolyte disrupts but does not prevent the correct operation of graphite. A decrease in the charge capacities is expected when considering the current peaks D and E. LiF seems to alter stages D and E in the lithium insertion. In the case of NMC electrode, the behavior observed in Fig. 4 (cycles 1 and 2) clearly shows a poor activation of the material whose stability is reduced to 4.2 V. Similarly, the mean current during charge–discharge phenomena is significantly lower than the one observed in the case of the reference electrolyte.

The presence of salts at the interface plays an important role in charge transfer resistance and diffusion of lithium ions in solution. To verify this aspect, we carried out electrochemical impedance tests at different stages of charging electrodes. Cycling was performed in the presence of LiOH and Li_2O, described in literature as the most harmful SEI salts towards battery functioning. In Fig. 5, we compare Nyquist plots obtained during the Li intercalation. Prior to the impedance spectroscopy tests, electrodes were stabilized by several galvanostatic charge–discharge cycles. Each impedance spectrum was measured while the electrode was in equilibrium before full charge or discharge state. Sets of plots reported in Fig. 5 are well resolved spectra in which a clear separation of the various time constants related to the Li^+ insertion processes is observed.

The high frequency semicircle relates to Li-ion migration through the SEI, and the medium frequency semicircle relates to charge transfer at the surface of the active material [29]. The low frequency slope that appears as a 'Warburg' type element reflects the solid state diffusion of lithium into the graphite (red curve), while at the very low frequencies, the steep line in these impedance spectra reflects the capacitive behavior of these electrodes, namely the accumulation of lithium in the graphite (i.e. the Li^+ insertion capacity at each potential). As shown in Fig. 5, all spectra contain a high frequency pronounced semicircle, which can be assigned to charge transfer resistance, and a very short straight line with a 45° slope from the real axis in the low frequency region, which reflects the solid-state Li^+ diffusion into the active mass. Furthermore, the impedance of the electrodes in the presence of LiOH (Fig. 5a) is much higher than that measured in the Li_2O solutions in the same conditions (Fig. 5b). This effect is accentuated in the case of the graphite electrode.

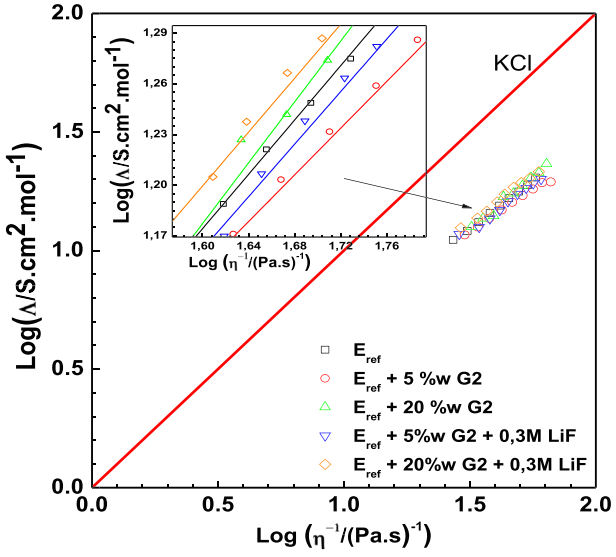

Fig. 2. Evolution of Walden plots of electrolytes with G2 and LiF addition.

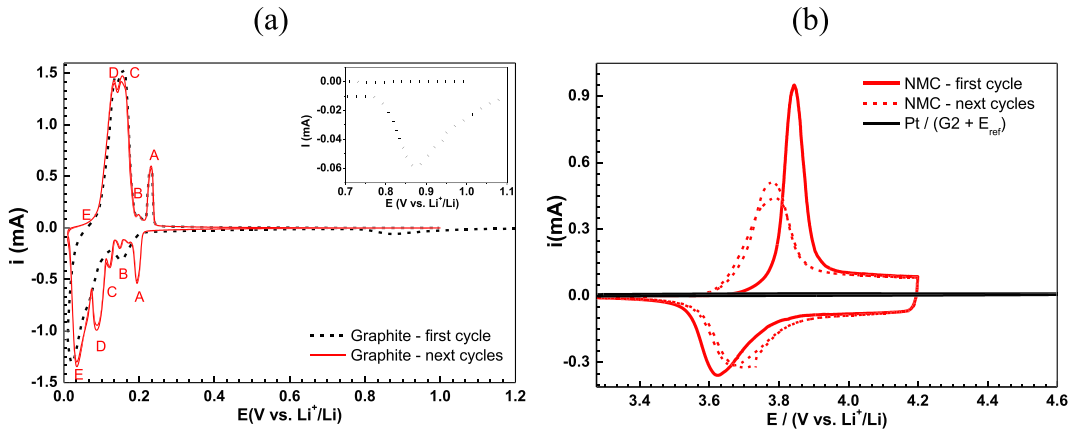

Fig. 3. Cyclic voltammetry on E_{ref} at scan rate of 10 μV s^{-1} on graphite (a) and NMC (b) electrodes (first cycle in dash), in insert the SEI formation at first cycle on graphite. Stability of (E_{ref} + G2) on platinum (b).

Table 2
Potentials of intercalation and de-intercalation of lithium in graphite corresponding to Fig. 3 and according to J.R. Dahn publication [29].

Peaks	A	B	C	D	E
Phase composition [1]	1′ + 4	4, 3	3 + 2L	2L + 2	2 + 1
Insertion potential (V)	0.185	0.143	0.113	0.075	0.034
De-insertion potential (V)	0.233	0.206	0.189	0.164	0.134

The charge–discharge curves of the cell are shown in Fig. 6 in the presence of LiOH and Li_2O salts in excess in the E_{ref}. The cell exhibited stable charge–discharge cycling behavior for over 30 cycles at C/10 regime. The first charge and discharge capacities are respectively close to (352 and 150) mA h g^{-1}, which are close to the theoretical capacities of graphite and NMC and similar to those obtained with E_{ref} (see Fig. 7). The coulombic efficiency of the first cycle is close to 87%, however the charge–discharge capacity decreased after the 2nd cycle and the efficiency becomes higher than 95%. Discharge capacities of (208 and 240) mA h g^{-1}, respectively in the case of LiOH and Li_2O at graphite and below 80 mA h g^{-1} at NMC are retained after 10 cycles, suggesting that considerable degradation of the SEI interface takes place upon repeated charge/discharge cycles. This result is in agreement with impedance data presented in Fig. 5.

The cycling performance of half-type cells based on graphite and NMC materials with electrolytes containing different lithium salts LiX in the classical E_{ref} is shown in Fig. 7 and compared to that obtained using the classical electrolyte E_{ref} at room temperature. Lithium salts were added until their saturation into the reference electrolyte. While, the effect of LiF salt on electrolyte performances has been tested at two concentrations: e.g. at 0.1 M and 0.3 M in E_{ref}, the latter corresponding to the LiF saturation limit in E_{ref} at room temperature.

As shown in Fig. 7a, the cell capacity with 0.1 M LiF, Li_2CO_3 and $LiOCH_3$ is slightly higher than that of standard electrolyte E_{ref}. Capacity values of 370 mA h g^{-1} for Li_2CO_3 and $LiOCH_3$ and 360 mA h g^{-1} for 0.1 M LiF were obtained after 10 cycles, respectively. Whereas the cells cycling performances with LiOH, Li_2O, and 0.3 M LiF-based electrolytes are seriously deteriorated, for example, less than 2/3 of initial capacity is retained in the case of Li_2O after 10 cycles. Finally, the capacity and capacity retention were 341.5 mA h g^{-1} and 98.7%, respectively after 10 cycles when $LiOC_2H_5$ is added into E_{ref}. This result suggests that SEI lithium salts may be separated in two different groups, according to their impact on cycling. In the first one, salts are capable to form a dense and steady SEI film at graphite electrode, with slightly positive or no impact on cycling capacity; this group comprises Li_2CO_3, $LiOCH_3$ and $LiOC_2H_5$ species. The second group is composed of LiOH and Li_2O. These components deteriorate the electrolyte cyclability and

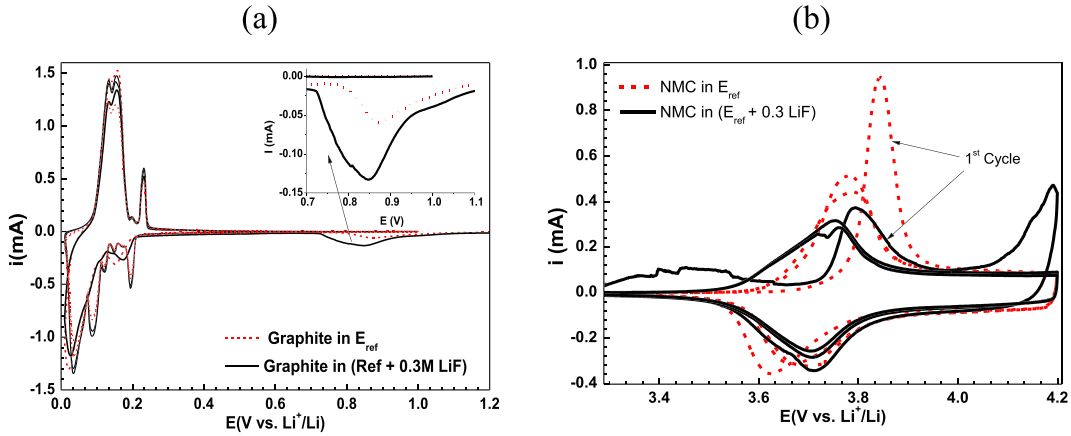

Fig. 4. Comparative cyclic voltammetry on (E_{ref} + G2) (solid line) and E_{ref} (dash line) at scan rate of 10 μV s^{-1} of graphite (a) and NMC (b) electrodes, in insert the SEI formation at first cycle on graphite.

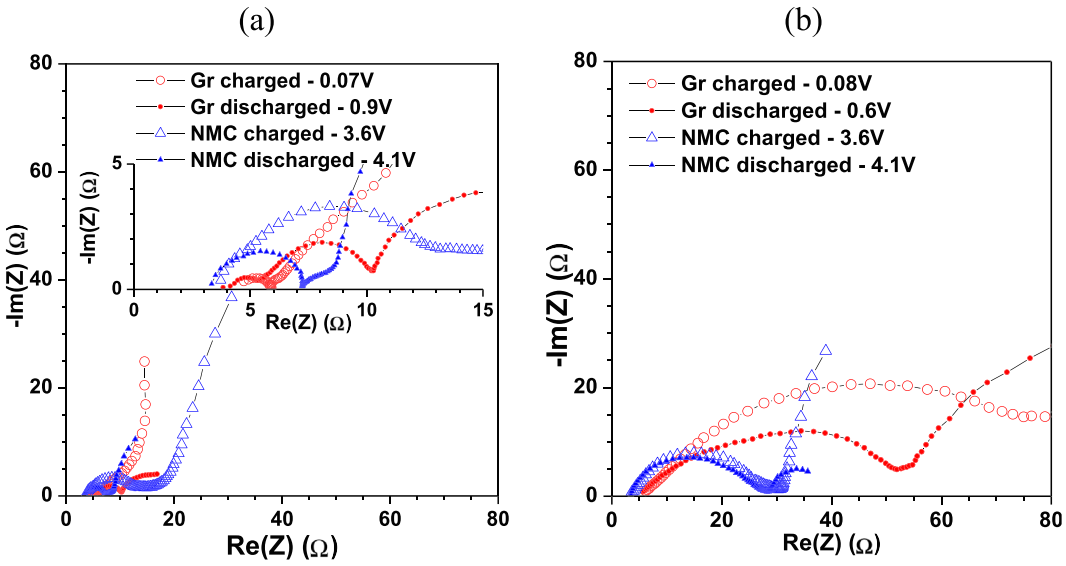

Fig. 5. Impedance spectra presented as Nyquist plots measured with graphite, NMC and complete cell in (a) EC/PC/3DMC (w/w) + 1 M $LiPF_6$ + Li_2O saturated, and (b) EC/PC/3DMC (w/w) + 1 M $LiPF_6$ + LiOH saturated solutions. Spectra were measured at equilibrium potentials (vs. Li/Li^+).

increase SEI resistance, resulting in a capacity reduction close to 30–40%. The LiF effect depends on its concentration: below a concentration close to 0.25 M, its impact is beneficial on E_{ref}, for higher concentration up to its saturation in E_{ref} (0.3 M) damaging effects are observed.

In Fig. 7b, we report cycling results obtained by using the same salts and the NMC electrode. The second group of detrimental salts is the same, namely LiOH, Li_2O and 0.3 M LiF. Capacities vary between (50 and 65) mA h g^{-1}. Results for the first group, composed of favorable salts (0.1 M LiF, Li_2CO_3, $LiOCH_3$ and $LiOC_2H_5$), are more dispersed and below that obtained for the reference electrolyte capacity (e.g. 160 mA h g^{-1}). For example, capacity values close to (95, 108, 113 and 120) mA h g^{-1} are obtained by adding 0.1 M LiF, Li_2CO_3, $LiOCH_3$ and $LiOC_2H_5$ in E_{ref}, respectively. These results show that all studied lithium salts have a negative impact on the NMC electrode, which is more reactive than graphite. This phenomenon leads to a decrease in capacity, from 35% ($LiOC_2H_5$) up to 85% (Li_2O) of the reference capacity.

3.2.2. *Impact of glyme on the cyclability in the presence of lithium salt*

Glymes have high donor numbers and relatively strong Lewis basicity due to the lone pairs on oxygen atoms in their structure, which results in a high ability to chelate lithium salts through strong solvation to Li^+. Recently, the equimolar complexes of glymes and Li salts were used as electrolytes for 4 V class lithium batteries [30]. We tested herein the effect of glyme addition (G2, G3 and G4) in E_{ref} containing 0.3 M LiF on the performance of graphite or NMC electrodes. This formulation was chosen because this LiF composition in solution leads to the larger decrease of electrolyte performances, as demonstrated above. Generally two G2 molecules are needed to chelate a Li^+, but the presence of fluorine prevents easy chelation of lithium by two molecules of G2 as described in the literature [25]; therefore we assume herein that only one G2 molecule is required to chelate a LiF species as shown in Scheme 1. For the following experiments reported in this work, we added an equivalent amount of glyme (G2, G3 or G4) to complex LiF i.e. 0.3 M of glyme in E_{ref}.

We first investigated the effect of the presence of glyme in the reference electrolyte E_{ref}, as well as of the glyme structure, G*n*

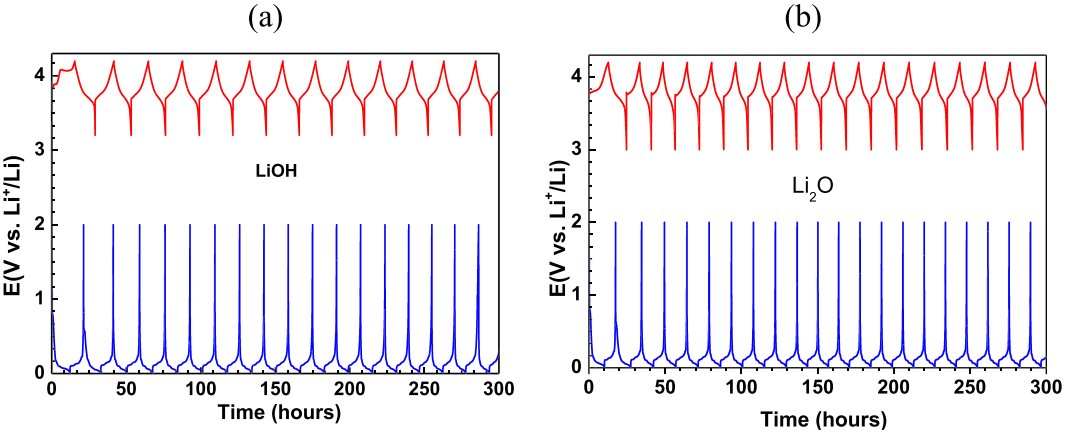

Fig. 6. Galvanostatic cycling of reference electrolyte with a lithium salt LiOH (a) or Li_2O (b) in half-cell configuration.

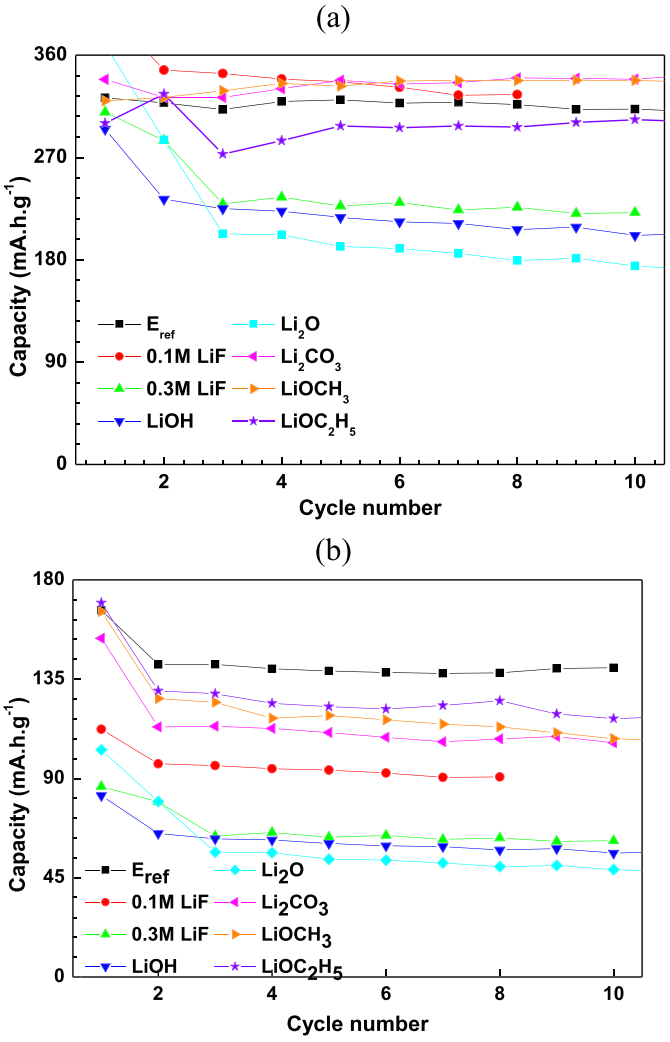

Fig. 7. Capacity evolution with (a) graphite and (b) NMC electrodes of EC/PC/3DMC + 1 M $LiPF_6$ (Ref) electrolyte by adding an SEI lithium salt.

($n = 2$, 3 and 4) on the capacity of the electrolyte. Fig. 8 shows that whatever the glyme structure, the addition of glyme in E_{ref} decreases its discharge capacity of graphite. Deterioration of performance is even more pronounced by increasing the glyme chain length: G4 > G3 > G2. With G4, this deterioration reaches 60% of

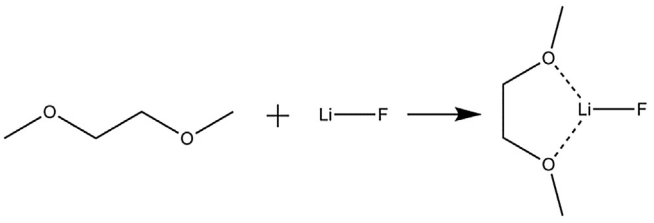

Scheme 1. Schematic representation of the chelation of LiF by G2.

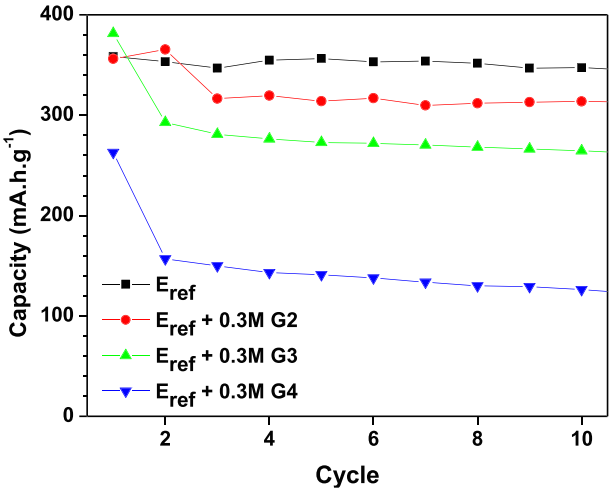

Fig. 8. Capacity evolution with graphite electrode of EC/PC/3DMC + 1 M $LiPF_6$ (Ref) electrolyte by adding 0.3 M glyme (G2, G3 or G4).

the initial capacity. These results can be interpreted as a strong complexation of free lithium ions by glyme molecules which decreases their availability for the insertion/de-insertion process. It is therefore not surprising that G4, which has a chelating power two times higher than that of G2, exhibits a more pronounced negative effect on electrolyte capacity, as the deterioration of performance seems to be two more times pronounced than that observed by adding G2 in E_{ref}.

These observations are reinforced by the complex impedance measurements performed in presence of LiX, with and without glymes, as shown in Fig. 9b. From which, it appears that the addition of G2 reduces transfer resistance due to polarization, related to

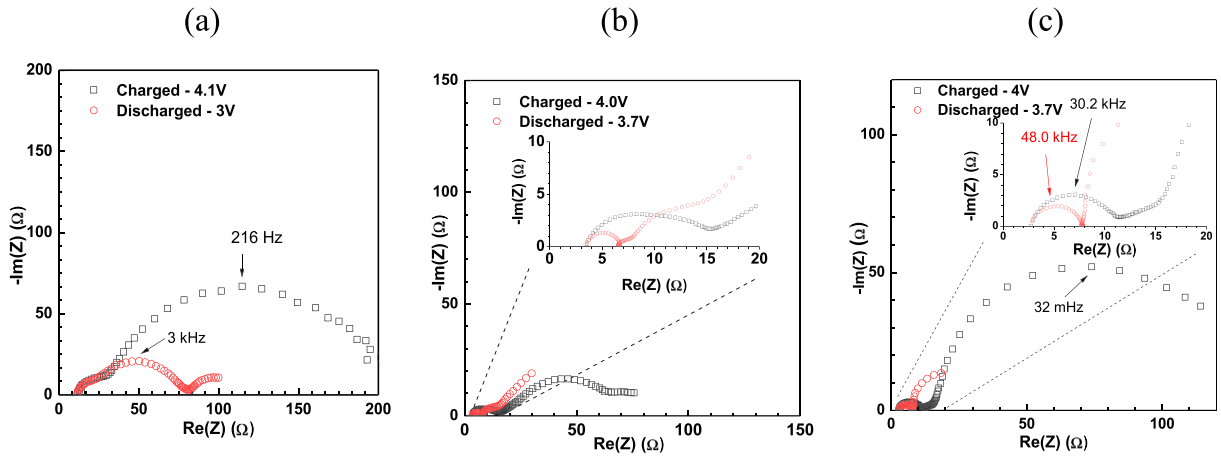

Fig. 9. Impedance spectra presented as Nyquist plots measured with graphite and NMC (full cell) electrodes in (a) EC/PC/3DMC + 1 M $LiPF_6$, (b) EC/PC/3DMC + 1 M $LiPF_6$ + 0.3 M G2, (c) EC/PC/3DMC + 1 M $LiPF_6$ + 0.3 M G2 + 0.3 M LiF. The spectra were measured at equilibrium potentials (vs. Li/Li^+).

Li-ion migration through the SEI and diffusion of ions in the active material. This fact is more visible without LiF, as in this case the resistance drops from 200 Ω (E_{ref}, Fig. 9a) to 130 Ω (E_{ref} with G2 and LiF, Fig. 9c) and to 50 Ω (E_{ref} with G2 but without LiF, Fig. 9b). From this work, it appears, that the addition of G2 in an electrolyte containing already LiF salt increases the resistance in comparison with an electrolyte without LiF salt. In other words, G2 molecules chelate LiF species rather than Li^+ cations from $LiPF_6$, in these solutions, and in fact G2 molecules stop to reduce the mobility of Li^+ as observed in the absence of LiF salt. Finally, this observation is further validated by the fact that electrolyte containing both G2 and LiF has a behavior closer to that observed with E_{ref}.

There are distinct differences between the glyme–LiF equimolar complexes and conventional lithium salts LiX (X = PF_6, TFSI, BF_4 …). In the latter, the Li^+ cation is involved in the formation of a $[Li(glyme)_n]^+$ cation [31], due to the high dissociation and high concentration of the salt. Furthermore, the glyme/LiF salt equimolar complexes exhibit lower stability than glyme/Li salt solutions containing excess Li^+. Because of the donation of lone pairs of ether oxygen to the Li^+ cation, it appears that the extraction of electrons from the lone pairs of $[Li(glyme)_n]^+$ complex cations becomes more difficult than that of free glyme or glyme/LiF complexes. Therefore, the glyme/Li salt equimolar complexes are presumed to be resistive against insertion of Li^+, and they are thought to decrease the performance of electrolytes.

When considering the CVs (Fig. 10) obtained during the first three cycles on graphite electrode in an electrolyte composed of the ternary mixture of E_{ref} with 0.3 M LiF and 0.3 M G2, we observe that the SEI layer formed during the first cycle is larger than that obtained in the case of free G2 and LiF based electrolyte, as the current involved in the process at 0.9 V vs. Li^+/Li is higher: 0.21 mA.

The cyclability of graphite was then tested in the presence of G2, G3 and G4 together with saturated electrolyte in 0.3 M LiF in E_{ref}: e.g. EC/PC/3DMC + 1 M $LiPF_6$. Results presented in Fig. 11 show that, whatever the glyme structure, the simultaneous presence of LiF and glyme in E_{ref} improves the cyclability of the solution. However, this improvement is more pronounced in the case of G4. Indeed, the glyme complexing power is harmful when the electrolyte contains only $LiPF_6$ ions in solution. This effect is even more visible in the case of G4. It is clear that the proportion of the ether bonding sites complexing lithium ions is directly related to their ability to complex lithium cations. When LiF is added to the mixture E_{ref} + G*n*, the preferred complexation of LiF by G*n* therefore leads to the release of Li^+ ions which may be inserted freely in the structure of graphite, as

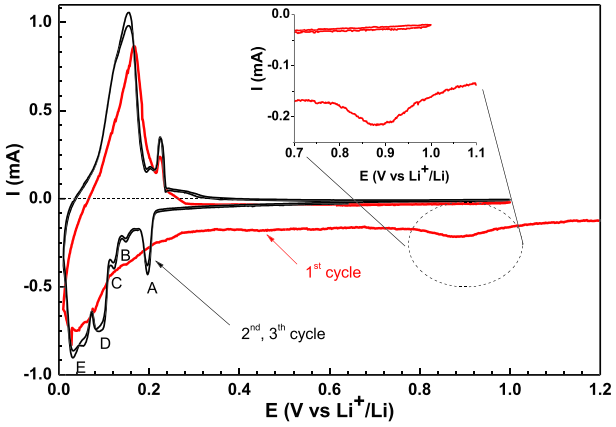

Fig. 10. Cyclic voltammetry at scan rate of 10 μV s^{-1} of graphite electrode in EC/PC/3DMC + 1 M $LiPF_6$ + 0.3 M LiF + 0.3 M G2 (in insert the SEI formation at first cycle on graphite).

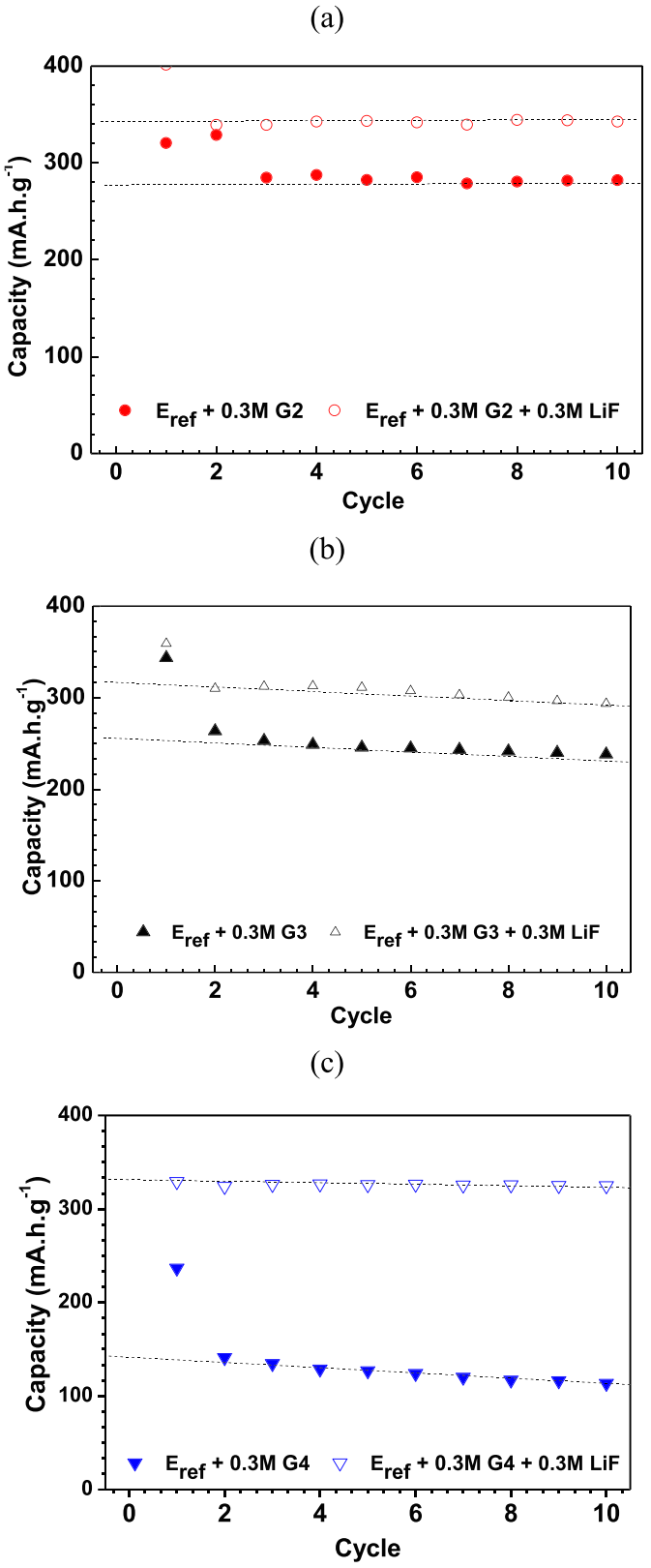

Fig. 11. Capacity evolution with graphite electrode of EC/PC/3DMC + 1 M $LiPF_6$ (Ref) electrolyte by adding 0.3 M glyme G2 (a), G3 (b) or G4 (c) with presence or absence of 0.3 M LiF in solution.

Table 3
Comparison of capacities on graphite electrode depending of the glyme structure added in the solution of LiF + EC/PC/3DMC + 1 M $LiPF_6$.

	Capacity (mA h g^{-1}) in E_{ref} with 0.3 M LiF	Capacity (mA h g^{-1}) in E_{ref} with 0.3 M G*n*	Capacity (mA h g^{-1}) in E_{ref} + 0.3 M LiF with 0.3 M G*n*
G2	260	284	342
G3	260	241	298
G4	260	116	325

observed in the case of "pure" E_{ref}. Herein, the presence of G2 helps to dissociate poly-associated $(LiF)_n$ molecules as octopoles and quadrupole ones [32], as already demonstrated during our previous works. This dissociation prevents then the salt precipitation on the SEI. At the same time, it does not inhibit in any way the availability of Li^+ ions from $LiPF_6$.

Table 3 shows the increases in capacity when adding G*n* to the reference electrolyte containing 0.3 M LiF. Improved performance when adding G*n* reached 30% of the initial capacity in the presence of 0.3 M LiF, for example. These results show also that it is possible to avoid the negative effect of LiF precipitation by adding an equivalent amount of glyme, because glyme molecules complex preferentially the lithium ions, and as a result, their aggregation in solution is then prevented. These investigations need to be extended to other salts that induce negative effects of the passivation layer as LiOH and Li_2O [33]. This is the subject of an ongoing study performed to date in our laboratory.

Fig. 11 shows comparison of capacities on graphite electrode of reference electrolyte with 0.3 M glyme (G2, G3 or G4) and with or without 0.3 M LiF. The longest the glyme chain is, the lower the capacity of the solution is. Indeed, G4 presents the lowest capacity of all investigated glyme solutions (around 110 mA h g^{-1}). The addition of LiF at equimolar concentration of G*n* clearly improves the electrolyte performances especially in the case of G4. These values are reported herein in Table 3.

4. Conclusion

Glymes exhibit attractive physico-chemical properties for electrolytes in lithium-ion batteries, particularly G2 which has low viscosity and good properties to insure the electrolyte safety. Moreover, according to the Walden classification, G2 does not have a strong impact on the ionicity of the solution. The presence of lithium salts in solution impact on cycling ability by modifying the SEI structure. LiOH, Li_2O and 0.3 M LiF have the worst effect on both graphite and NMC electrodes (loss of respectively 1/3 and 2/3 of the reference capacity in comparison with the reference electrolyte: EC/PC/3DMC (w/w) + 1 M $LiPF_6$, denoted E_{ref}). The other solution tested containing (0.1 M LiF, Li_2CO_3, $LiOCH_3$ or $LiOC_2H_5$) salt dissolved in E_{ref} perform better on NMC electrode than previous salts and present capacity values on graphite electrode near to the reference electrolyte one.

The addition of glymes in the reference electrolyte tends to decrease the solution capacity depending on their chain length. But with the presence of both glyme and LiF salt in the reference electrolyte, it inhibits the detrimental side reactions by chelating LiF and preventing its aggregation. In conclusion, glymes are effective electrolyte additives and their complexing ability towards SEI compounds will be the subject of future investigations in our laboratory to optimize battery performances.

Acknowledgments

This research was supported by CNES and CEA Le Ripault. The authors would like to thank also SAFT (France) for providing the electrode materials.

References

[1] E. Peled, J. Electrochem. Soc. 126 (1979) 2047–2051.
[2] P. Verma, P. Maire, P. Novák, Electrochim. Acta 55 (2010) 6332–6341.
[3] A.M. Andersson, D.P. Abraham, R. Haasch, S. MacLaren, J. Liu, K. Amine, J. Electrochem. Soc. 149 (2002) A1358–A1369.
[4] H. Bryngelsson, M. Stjerndahl, T. Gustafsson, K. Edström, J. Power Sources 174 (2007) 970–975.
[5] J. Jones, M. Anouti, M. Caillon-Caravanier, P. Willmann, P.-Y. Sizaret, D. Lemordant, Fluid Phase Equilib. 305 (2011) 121–126.
[6] R. Dedryvère, H. Martinez, S. Leroy, D. Lemordant, F. Bonhomme, P. Biensan, D. Gonbeau, J. Power Sources 174 (2007) 462–468.
[7] S. Leroy, H. Martinez, R. Dedryvère, D. Lemordant, D. Gonbeau, Appl. Surf. Sci. 253 (2007) 4895–4905.
[8] P. Arora, R.E. White, M. Doyle, J. Electrochem. Soc. 145 (1998) 3647–3667.
[9] D. Aurbach, B. Markovsky, A. Shechter, Y. Ein-Eli, H. Cohen, J. Electrochem. Soc. 143 (1996) 3809–3820.
[10] R. Dedryvère, S. Laruelle, S. Grugeon, L. Gireaud, J.-M. Tarascon, D. Gonbeau, J. Electrochem. Soc. 152 (2005) A689–A 696.
[11] S.-H. Kang, D.P. Abraham, A. Xiao, B.L. Lucht, J. Power Sources 175 (2008) 526–532.
[12] H.-L. Zhang, F. Li, C. Liu, J. Tan, H.-M. Cheng, J. Phys. Chem. B 109 (2005) 22205–22211.
[13] D. Aurbach, Y. Ein-Eli, O. Chusid, Y. Carmeli, M. Babai, H. Yamin, J. Electrochem. Soc. 141 (1994) 603–611.
[14] A.N. Dey, B.P. Sullivan, J. Electrochem. Soc. 117 (1970) 222–224.
[15] M.N. Richard, J.R. Dahn, J. Electrochem. Soc. 146 (1999) 2068–2077.
[16] D. Aurbach, J. Power Sources 89 (2000) 206–218.
[17] Y.-K. Choi, K. Chung, W.-S. Kim, Y.-E. Sung, S.-M. Park, J. Power Sources 104 (2002) 132–139.
[18] J.-S. Shin, C.-H. Han, U.-H. Jung, S.-I. Lee, H.-J. Kim, K. Kim, J. Power Sources 109 (2002) 47–52.
[19] K. Tasaki, S.J. Harris, J. Phys. Chem. C 114 (2010) 8076–8083.
[20] I. Geoffroy, P. Willmann, K. Mesfar, B. Carré, D. Lemordant, Electrochim. Acta 45 (2000) 2019–2027.
[21] T. Inose, D. Watanabe, H. Morimoto, S.-I. Tobishima, J. Power Sources 162 (2006) 1297–1303.
[22] D.-J. Lee, J. Hassoun, S. Panero, Y.-K. Sun, B. Scrosati, Electrochem. Commun. 14 (2012) 43–46.
[23] K. Yoshida, M. Nakamura, Y. Kazue, N. Tachikawa, S. Tsuzuki, S. Seki, K. Dokko, M. Watanabe, J. Am. Chem. Soc. 133 (2011) 13121–13129.
[24] Y. Choquette, G. Brisard, M. Parent, D. Brouillette, G. Perron, J.E. Desnoyers, M. Armand, D. Gravel, N. Slougui, J. Electrochem. Soc. 145 (1998) 3500–3507.
[25] A.M. Christie, C.A. Vincent, J. Phys. Chem. 100 (1995) 4618–4621.
[26] M.r.m. Anouti, M. Caillon-Caravanier, Y. Dridi, H. Galiano, D. Lemordant, J. Phys. Chem. B 112 (2008) 13335–13343.
[27] W. Paul, Z. Phys. Chem. 55 (1906) 207–249.
[28] J.R. Dahn, Phys. Rev. B 44 (1991) 9170–9177.
[29] J.R. Macdonald, Impedance Spectroscopy Theory, Experiment, and Applications, John Wiley & Sons, 2005.
[30] S. Seki, N. Serizawa, K. Takei, K. Dokko, M. Watanabe, J. Power Sources 243 (2013) 323–327.
[31] K. Ueno, K. Yoshida, M. Tsuchiya, N. Tachikawa, K. Dokko, M. Watanabe, J. Phys. Chem. B 116 (2012) 11323–11331.
[32] J. Jones, M. Anouti, M. Caillon-Caravanier, P. Willmann, D. Lemordant, Fluid Phase Equilib. 285 (2009) 62–68.
[33] S. Chattopadhyay, A.L. Lipson, H.J. Karmel, J.D. Emery, T.T. Fister, P.A. Fenter, M.C. Hersam, M.J. Bedzyk, Chem. Mater. 24 (2012) 3038–3043.